Turk J Chem
36 (2012) , 25 – 36.

doi:10.3906/kim-1106-50

Synthesis and structural and electrochemical characterization of novel macrocyclic *vic*-dioxime ligand and its mononuclear transition and nontransition metal complexes

Pervin DEVECİ[1], Bilge TANER[1], Zeynel KILIÇ[2], Ali Osman SOLAK[2,3], Emine ÖZCAN[1,*]

[1] *Department of Chemistry, Faculty of Science, Selçuk University, Konya-TURKEY*
e-mail: emineozcan@hotmail.com

[2] *Department of Chemistry, Faculty of Science, Ankara University, Tandoğan, Ankara-TURKEY*

[3] *Department of Chemical Engineering, Faculty of Engineering, Kyrgyz-Turk Manas University, CAL Campus, Bishkek-KYRGYZSTAN*

Received: 22.06.2011

The reaction of N-(4-aminophenyl)aza-15-crown-5 (**1**) with *anti*-chlorophenylglyoxime (**2**) produces a novel azacrown ether containing *vic*-dioxime, N-(4-aminophenyl)aza-15-crown-5-phenylglyoxime (LH_2). LH_2 reacts with Ni(II), Cu(II), Co(II), Cd(II), and Zn(II) ions to yield the mononuclear transition and nontransition metal complexes $[M(LH)_2]$ (M = Ni and Cu), $[M(LH)_2(H_2O)_2]$ (M = Co), and $[M(LH)(H_2O)(Cl)]$ (M = Cd and Zn). The structural features of LH_2 were studied using several techniques including elemental analysis, Fourier transform infrared spectroscopy (FT-IR), ultraviolet visible (UV-Vis), mass spectrometry (MS), 1-dimensional (1D) ^{1}H-NMR and ^{13}CNMR, distortionless enhancement by polarization transfer (DEPT) 2-dimensional (2D) heteronuclear single-quantum coherence (HSQC), and heteronuclear multiple-bond correlation (HMBC) techniques. The structures of the complexes were confirmed by elemental analyses and with the use of magnetic susceptibility measurements, MS, UV-Vis, FT-IR, ^{1}H-NMR, and ^{13}C-NMR techniques. The redox behaviors of the ligand and its complexes were verified with cyclic voltammetry (CV) at a glassy carbon (GC) electrode in 0.1 M tetrabutylammoniumtetrafluoroborate (TBATFB) in dimethyl sulfoxide (DMSO).

Key Words: *vic*-Dioxime, azacrown ether, transition metal complexes, mass spectroscopy, cyclic voltammetry

*Corresponding author

Introduction

The design and synthesis of new macrocyclic *vic*-dioxime ligands with heteronucleating donor atoms is closely connected to promising applications in different areas. Various macrocyclic *vic*-dioxime ligands, as well as their open-chain counterparts, have been synthesized and characterized for a variety of purposes.[1–4] The presence of mildly acidic hydroxyl groups and moderately basic nitrogen atoms makes *vic*-dioxime an amphoteric ligand that forms corrin-type square-planar, square-pyramidal, and octahedral complexes with transition metal ions such as Ni(II), Cu(II), Co(II), and Pd(II).[5] The chemistry of these complexes has attracted much attention, due to their applications in important chemical processes in medicine[6] extractions[7,8] bioorganic systems[9,10] and polymers.[11,12] The physical and chemical properties of *vic*-dioximes and their complexes may be improved by adding functional groups such as crown ethers, azacrown ethers, calix pyrroles, ferrocenes, tetrathiamacrocycles or N_2O_2 macrocycles and dendritic groups.[13–15] To increase the low solubilities of the *vic*-dioxime complexes and to address interest in the synthesis of azacrown-based compounds, the synthesis and characterization of the azacrownlinked *vic*-dioxime ligand and its Cd(II), Zn(II), Ni(II), Cu(II), and Co(II) complexes are herein reported. Due to recent growth in interest in the electrochemistry of macrocyclic complexes, the electrochemical properties of all of the compounds were studied using cyclic voltammetry (CV), including oxidation and reduction processes that involved both central atoms and ligands. Our future strategy will involve the preparation of alkaline and alkaline-earth metal cations to this ligand in hopes of determining their structures.

Experimental

Materials and measurements

N-(4-aminophenyl)aza-15-crown-5 (**1**)[16] and *anti*-chlorophenylglyoxime (**2**)[17] were prepared according to procedures reported in the literature. All other chemicals were received from Merck or Sigma-Aldrich and used as supplied. Silica gel (70-230 mesh) was used for chromatographic separations. All organic solvents were dried and purified by means of the usual methods. All processes performed in aqueous media, as well as the preparation of aqueous solutions, were carried out using ultrapure water with a resistance of approximately 18.3 MΩ cm^{-1} (Human Power 1^+ Scholar Purification System, Human Corporation). Before electrochemical experiments, solutions were purged with pure argon gas (99.999%) for at least 10 min, and an argon atmosphere was maintained over the solution during experiments. Elemental analyses were performed on a CHNSO analyzer. NMR experiments were performed with a Varian Unity INOVA 500 spectrometer using a 5-mm ID-PFG probe at 298.15 K. Samples were dissolved in dimethyl sulfoxide (DMSO). Chemical shifts were reported in ppm relative to TMS for ^{1}H- and ^{13}C-NMR spectra. ^{1}H-NMR, ^{13}C-NMR, and heteronuclear single-quantum coherence (HSQC) and heteronuclear multiple-bond correlation (HMBC) NMR spectra were obtained at a base frequency of 125.71 MHz for ^{13}C and 499.95 MHz for ^{1}H nuclei. Two-dimensional gradient HSQC and HMBC techniques were measured using the standard pulse programs provided by Varian. The spectra were acquired with 512 increments in the F1 dimension and 2048 data points in the F2 dimension. The IR spectra of solid samples were recorded on a PerkinElmer Spectrum 100 Fourier transform infrared spectroscopy (FT-IR) spectrometer (Universal/ATR Sampling Accessory). Ultraviolet-visible (UV-Vis) spectra were obtained on Shi-

madzu UV-1700 spectrophotometers. Melting points were determined using an electrothermal apparatus and were uncorrected. Magnetic moments of the complexes were measured using a Sherwood Scientific Model MX1 Gouy magnetic susceptibility balance at room temperature with $Hg[Co(SCN)_4]$ as the calibrate; diamagnetic corrections were calculated from Pascal's constants. Mass spectrometry (MS) spectra were recorded on a Bruker MicrOTOF LC-MS spectrometer. Cyclic voltammograms were recorded on a CH Instruments electrochemical analyzer (model 600C series) equipped with a BAS C3 cell stand. The electrochemical cell was equipped with a bare glassy carbon (GC) disk (BAS Model MF-2012) with a geometric area of 0.027 cm^2 and a platinum auxiliary electrode. Electrochemical studies of the compounds were performed in a solution of 1 mM in 0.1 M tetrabutylammoniumtetrafluoroborate (TBATFB) in DMSO vs. Ag/Ag^+ (0.01 M $AgNO_3$) reference electrode, using CV with a scan rate of 200 mV s^{-1} between 1 V and –2.5 V. To prepare the Ag/Ag^+ (0.01 M $AgNO_3$) reference electrode, pure $AgNO_3$ was dissolved in 0.1 M TBATFB in acetonitrile to obtain a 0.01 M Ag^+ inner solution, and it was calibrated with ferrocene regularly.

Synthesis of the ligand: N-(4-aminophenyl)aza-15-crown-5-phenylglyoxime (LH_2)

A solution of **1** (0.47 g, 1.50 mmol) in diethyl ether (10 mL) was added to a stirred mixture of **2** (0.29 g, 1.50 mmol) and triethylamine (0.21 mL, 1.50 mmol) in diethyl ether (10 mL). The mixture was stirred at room temperature for 2 h in a N_2 atmosphere and monitored by thin-layer chromatography, using methanol. The solvent was evaporated and the residue was purified via column chromatography on silica gel, using methanol to give the *vic*-dioxime derivative (LH_2). Yield: 0.56 g (79%). Mp: 101 °C. Anal. Calc. for $C_{24}H_{32}N_4O_6$: C, 61.00; H, 6.83; N, 11.86%. Found: C, 61.10; H, 6.79; N, 11.78%. MS (fragments are based on the most abundant isotopes): m/z 473.930 $(MH)^+$ (Calc. 473.240). FT-IR (ν_{max}/cm^{-1}): 3246 (O–H), 3150 (N–H), 3030(C–$H_{arom.}$), 2980 (C–$H_{aliph.}$), 1618 (C=N), 1517 (C=C), 990 (N–O) cm^{-1}. ^{1}H-NMR (DMSO-d_6), δ (ppm): 3.37 (t, 4H, CH_2N), 3.46 (bs, 4H, CH_2O), 3.50 (bs, 4H, CH_2O), 3.54 (t, 4H, CH_2O), 6.70 (dd, 2H, ArH), 6.37 (dd, 2H, ArH), 7.28-7.26 (m, 3H, ArH), 7.40-7.42 (m, 2H, ArH), 7.69 (s, 1H, NH), 10.13 (s, 1H, OH), 11.54 (s, 1H, OH). ^{13}C-NMR (DMSO-d_6), δ (ppm): 57.30, 73.40, 74.43, 74.86, 75.64, 116.61, 128.92, 132.94, 134.34, 134.42, 136.80, 136.90, 148.90, 153.81, 154.01.

Synthesis of the complexes ($[Cd(LH)(H_2O)(Cl)]$, $[Zn(LH)(H_2O)(Cl)]$, $Ni(LH)_2$, $Cu(LH)_2$, $Co(LH)_2(H_2O)_2$)

A solution of $CdCl_2{\cdot}2H_2O$ (0.114 g, 0.50 mmol), $ZnCl_2$ (0.07 g, 0.50 mmol), $NiCl_2{\cdot}6H_2O$ (0.059 g, 0.25 mmol), $CuCl_2{\cdot}2H_2O$ (0.043 g, 0.25 mmol), or $CoCl_2{\cdot}6H_2O$ (0.059 g, 0.25 mmol) in water (5 mL) was added to a solution of LH_2 (0.24 g, 0.50 mmol) in methanol (5 mL) at room temperature. A distinct change in color and a decrease in the pH of the solution (3.5-4.0) were observed. While stirring at the same temperature, NaOH (1%) was added to increase the pH to 7. The reaction mixture was stirred for 30 min at room temperature. The precipitate was filtered off, washed several times with water, and then dried in vacuum.

[Cd(LH)(H_2O)(Cl)]

Yield: 0.091 g (57%). Mp: 298 °C. Anal. Calc. for $C_{24}H_{33}N_4O_7ClCd$: C, 45.22; H, 5.22; N 8.79. Found: C, 45.15; H, 5.20; N, 8.65%. MS (fragments are based on ^{110}Cd and ^{35}Cl): m/z 616.537 (M-[H_2O])$^+$ (Calc. 616.580). FT-IR (ν_{max}/cm^{-1}): 3261 (O–H), 3200 (N–H), 3020 (C–H $_{arom.}$), 2982 (C–H $_{aliph.}$), 1615 (C=N), 1516 (C=C), 973 (N–O). ^{1}H-NMR (DMSO-d_6), δ (ppm): 3.38 (s, 2H, H_2O), 3.45-3.55 (m, 20H, CH_2CH_2O, CH_2CH_2N), 6.37 (dd, 2H, ArH), 6.68 (dd, 2H, ArH), 7.27-7.40 (m, 5H, ArH), 7.72 (s, 1H, NH), 10.13 (s, 1H, OH). ^{13}C-NMR (DMSO-d_6), δ (ppm): 52.02, 68.73, 70.04, 70.13, 70.96, 111.73, 124.06, 132.37, 135.50, 135.52, 136.16, 136.81, 148.89, 151.36, 153.24.

[Zn(LH)(H_2O)(Cl)]

Yield: 0.051 g (33%). Mp: 156 °C. Anal. Calc. for $C_{24}H_{33}N_4O_7ClZn$: C, 48.82; H, 5.63; N, 9.49. Found: C, 48.70; H, 5.66; N, 9.40%. MS (fragments are based on ^{64}Zn and ^{35}Cl): m/z 589.529 (MH)$^+$ (Calc. 589.625). FT-IR (ν_{max}/cm^{-1}): 3265 (O–H), 3110 (N–H), 3028 (C–H$_{arom.}$), 2975 (C–H$_{aliph.}$), 1611 (C=N), 1516 (C=C), 983 (N–O) cm^{-1}. ^{1}H-NMR (DMSO-d_6), δ (ppm): 3.36 (s, 2H, H_2O), 3.47-3.56 (m, 20H, CH_2CH_2O, CH_2CH_2N), 6.39 (dd, 2H, ArH), 6.70 (dd, 2H, ArH), 7.29-7.43 (m, 5H, ArH), 7.75 (s, 1H, NH), 10.15 (s, 1H, OH). ^{13}C-NMR (DMSO-d_6), δ (ppm): 52.63, 68.74, 70.07, 70.16, 71.01, 111.73, 124.03, 132.40, 134.93, 135.59, 136.23, 136.81, 148.86, 152.91, 153.02.

Ni(LH)$_2$

Yield: 0.19 g (75%). Mp: 243 °C. Anal. Calc. for $C_{48}H_{62}N_8O_{12}Ni$: C, 57.55; H, 6.24; N, 11.19. Found: C, 57.52; H, 6.22; N, 11.12%. MS (fragments are based on ^{58}Ni): m/z 1001.769 (MH)$^+$ (Calc. 1001.392). FT-IR (ν_{max}/cm^{-1}): 3240 (O-H), 3148 (N–H), 3020 (C–H$_{arom.}$), 2980 (C–H$_{aliph.}$), 1762 (O–H$\cdots$O), 1608 (C=N), 1514 (C=C), 983 (N–O) cm^{-1}. ^{1}H-NMR (DMSO-d_6), δ (ppm): 2.63-3.53 (m, 40H, CH_2CH_2O and CH_2CH_2N), 6.04 (s, 2H, NH), 6.82-6.94 (m, 18H, ArH), 14.34 (s, 2H, O–H$\cdots$O). ^{13}C-NMR (DMSO-d_6), δ (ppm): 52.06, 67.93, 69.10, 69.50 70.36, 115.34, 128.68, 132.25, 135.30, 136.20, 137.40, 138.45, 143.50, 155.20, 156.05.

Cu(LH)$_2$

Yield: 0.19 g (74%). Mp: 165 °C. Anal. Calc. for $C_{48}H_{62}N_8O_{12}Cu$: C, 57.27; H, 6.21; N, 11.13. Found: C, 57.23; H, 6.25; N 11.16%. MS (fragments are based on ^{63}Cu): m/z 933.614 (MH-[CHN_2O_2])$^+$ (Calc. 933.383). FT-IR (ν_{max}/cm^{-1}): 3250 (O-H), 3150 (N–H), 3030 (C–H$_{arom.}$), 2985(C–H$_{aliph.}$), 1718 (O–H$\cdots$O), 1606 (C=N), 1513 (C=C), 983 (N–O) cm^{-1}.

Co(LH)$_2$(H_2O)$_2$

Yield: 0.17 g (65%). Mp: >300 °C. Anal. Calc. for $C_{48}H_{66}N_8O_{14}Co$: C, 55.54; H, 6.40; N 10.80. Found: C, 55.50; H, 6.47; N, 10.75%. MS (fragments are based on ^{59}Co): m/z 1001.998 (M-[2H_2O])$^+$ (Calc. 1001.382).

FT-IR (ν_{max}/cm^{-1}): 3261 (O–H), 3155 (N–H), 3025 (C–H $_{arom.}$), 2970 (C–H$_{aliph.}$), 1718 (O-H..O), 1600 (C=N), 1513 (C=C), 982 (N–O).

Results and discussion

Synthesis of the *vic*-dioxime ligand was accomplished with an acceptable yield (79%) by reacting **1**[16] with **2**[17] in diethyl ether (Scheme).

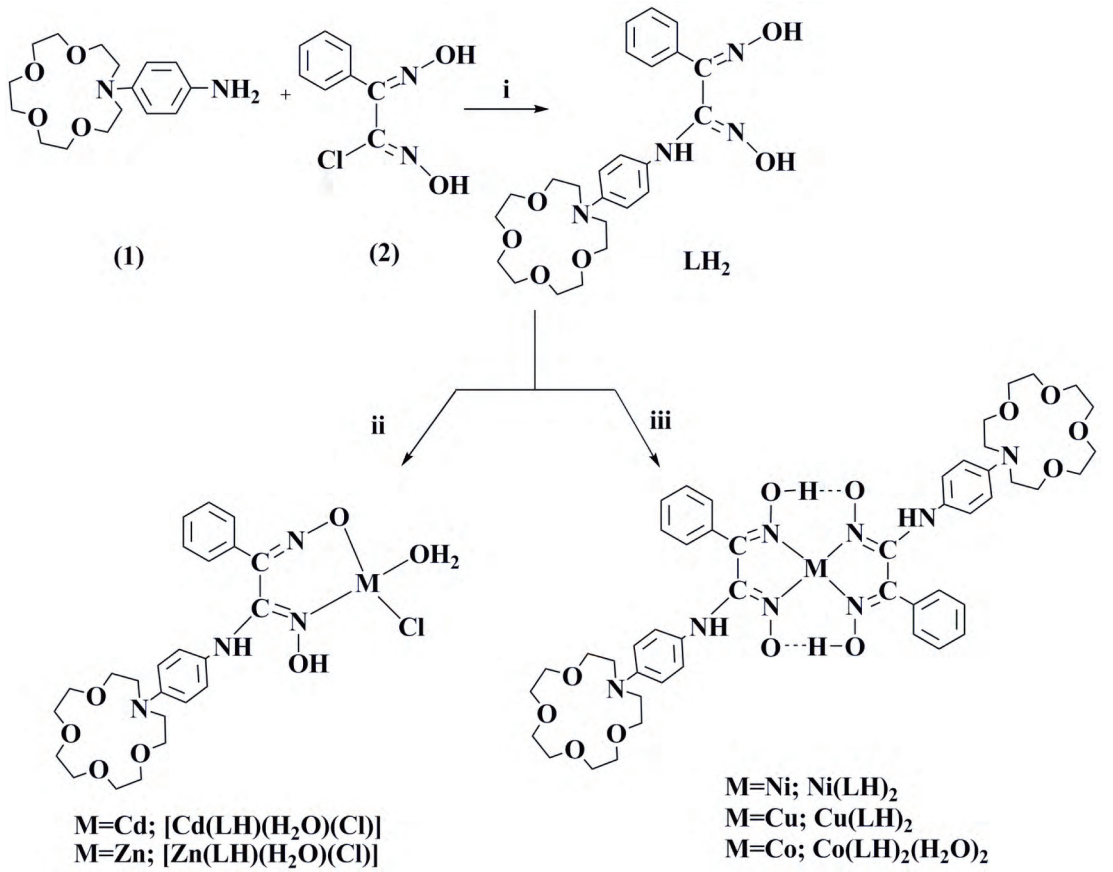

Scheme. Synthesis of LH_2 and its complexes $Ni(LH)_2$, $Cu(LH)_2$, $Co(LH)_2(H_2O)_2$, [Cd(LH)(H_2O)(Cl)] and [Zn(LH)(H_2O)(Cl)]; i): Et_2O, Et_3N, RT; ii): $CdCl_2 \cdot 2H_2O$ or $ZnCl_2$; (iii): $NiCl_2 \cdot 6H_2O$, $CuCl_2 \cdot 2H_2O$, or $CoCl_2 \cdot 6H_2O$.

Characterization of the *vic*-dioxime ligand

The structure proposed for LH_2 is consistent with the data obtained from elemental analyses, MS, 1D NMR (^{1}HNMR, ^{13}CNMR and distortionless enhancement by polarization transfer (DEPT)) and 2D NMR (HSQC and HMBC), UV-Vis, and FT-IR spectral studies. The FTIR spectrum of LH_2 shows no characteristic absorption assignable to the $-NH_2$ function in the starting material, but exhibits a broad resonance at 3246 cm^{-1}, which can be attributed to the O–H stretching of the hydroxyimino groups. It shows sharp and intense peaks at

1618 and 990 cm^{-1} which can be attributed to –C=N and N–O stretching vibrations respectively. The characteristic medium intensity stretching of C–H_{arom} and C–H_{aliph} vibrations was observed at 3030 and 2980 cm^{-1}, respectively. The electronic spectra for LH_2 and its complexes recorded in DMSO, are given in Figure S1 in the Supplementary Materials section. The electronic spectral data of the ligand exhibit 2 bands in the UV region. The band appearing at 281 nm is attributed to the $\pi \rightarrow \pi^*$ transition of the ligand. The band at around 332 nm can be assigned to the n$\rightarrow \pi^*$ transition of the –C=N group.[18] The mass spectra of LH_2 (Figure S2 in Supplementary Materials; fragments are based on the most abundant isotopes) shows a molecular ion peak at m/z 473.930 $(MH)^+$ (Calc. 473.240), confirming the formation of the desired compound. Removal of the hydroxyl ion resulted in a (MH-[OH])$^+$ species with a molecular ion peak at m/z 457.924 (Calc. 457.645). In the ^{1}H-NMR spectra of LH_2, a broad signal concerning the aromatic primary amine group disappeared, and a new chemical shift at 7.69 ppm was observed as a singlet that could be assigned to the –NH proton. The signals due to azacrown ether moiety were observed at 3.37-3.54 ppm. The aromatic ring protons were observed at 6.70 ppm (H_7) and 6.37 ppm (H_8) as 2 doublets of doublets (^3J = 8.88 Hz, ^4J = 1.78 Hz), and at 7.26-7.28 ppm ($H_{14,15}$) and 7.40-7.42 ppm (H_{13}) as 2 multiplets (Scheme S, Supplementary Materials). The chemical shifts of N–OH protons were observed at 10.13 ppm and 11.54 ppm as singlets. These 2 deuterium-exchangeable singlets correspond to 2 nonequivalent –OH protons, which also indicate the *anti*-configuration of the –OH groups relative to each other.[19,20] More detailed information about the structure of LH_2 was provided by performing a combination of ^{13}C-NMR, DEPT, HSQC NMR, and HMBC NMR experiments.

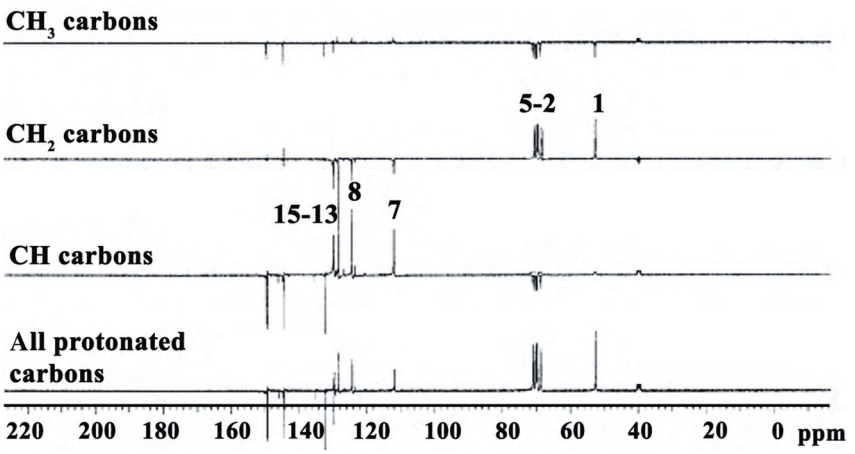

Figure 1. DEPT spectrum of LH_2 in DMSO-d_6.

The ^{13}C-NMR spectra of LH_2 show 15 different carbon atoms that are consistent with the proposed structure of the ligand on the basis of molecular symmetry. All of the ^{13}C-NMR chemical shifts for LH_2 are given in Table S in the Supplementary Materials section, along with the HMBC and HSQC correlations. The numbering scheme for the assignment of protons and carbons is depicted in Scheme S (Supplementary Materials). In the ^{13}C-NMR spectra of LH_2, the carbon resonance of the azomethine group was observed at 153.81 and 154.01 ppm and these 2 different frequencies for the oxime group confirm the *anti* form of the *vic*-dioxime ligand.[21,22] DEPT was used to better discriminate between different types of carbons present in the ligand. The DEPT spectrum (Figure S1) gives the –CH_2 peaks at 57.30, 73.40, 74.43, 74.86, and 75.64 ppm and the –CH peaks at 116.61, 128.92, 134.34, 134.42, and 136.90 ppm. The carbons recorded in ^{13}C-NMR but

nulled in DEPT are carbons without any attached hydrogens. More detailed information about the structure of the ligand is provided by the 2D HSQC and HMBC spectra (Figure 2 and 3), and all correlations are in accordance with the proposed structure.

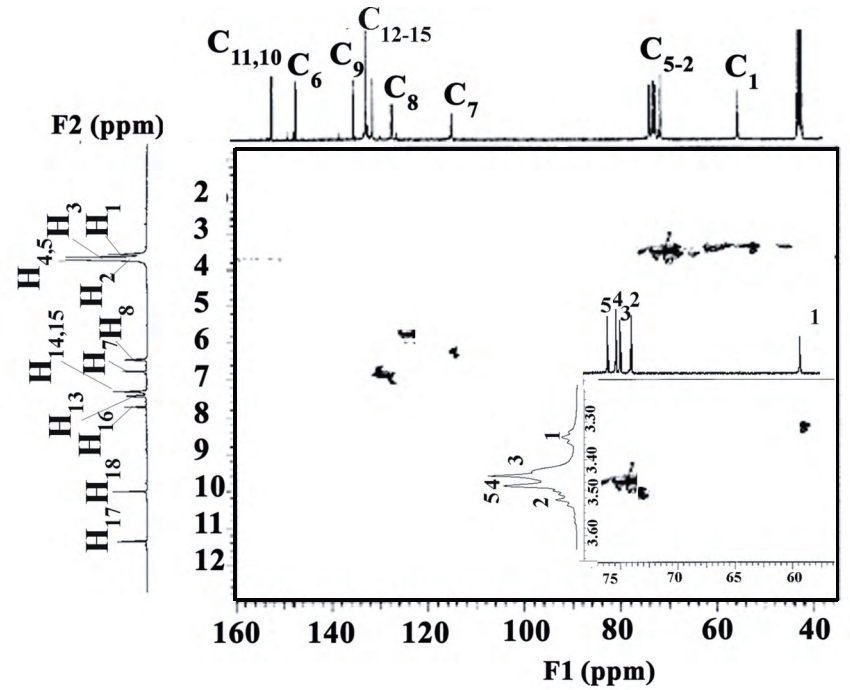

Figure 2. HSQC spectrum of LH_2 in DMSO-d_6 (expanded form of the azacrown ether region is shown in the box inset).

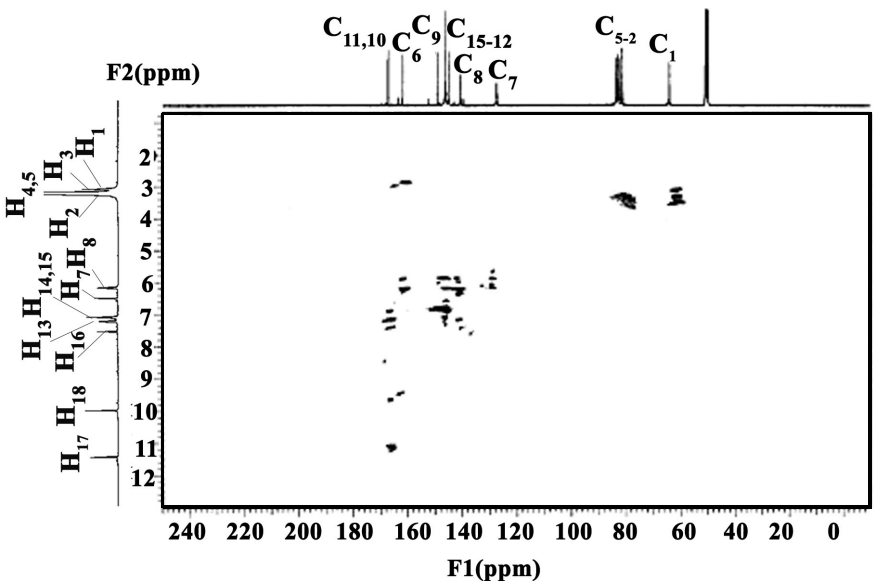

Figure 3. HMBC spectrum of LH_2 in DMSO-d_6.

Characterization of the *vic*-dioxime complexes

The mononuclear Cd(II), Zn(II) Ni(II), Cu(II) and Co(II) complexes were synthesized from the *vic*-dioxime derivative (LH_2) with a stoichiometric amount of $CdCl_2 2H_2O$, $ZnCl_2$, $NiCl_2 \cdot 6H_2O$, $CuCl_2 \cdot 2H_2O$, and $CoCl_2 \cdot 6H_2O$, respectively, in the presence of diethyl ether (Scheme). Both elemental analysis and mass spectral data showed that the metal-to-ligand ratio was 1:1 for compounds $[Cd(LH)(H_2O)(Cl)]$ and $[Zn(LH)(H_2O)(Cl)]$ and 1:2 for compounds $Ni(LH)_2$, $Cu(LH)_2$, and $Co(LH)_2(H_2O)_2$ The magnetic susceptibility values of the complexes show that the $Ni(LH)_2$, $[Cd(LH)(H_2O)(Cl)]$ and $[Zn(LH)(H_2O)(Cl)]$ are diamagnetic, while the $Cu(LH)_2$ and $Co(LH)_2(H_2O)_2$ compounds are paramagnetic. The measured values for the Cu(II) and Co(II) complexes were 1.73 and 3.85 BM, respectively. In the ^{1}HNMR spectra of $Ni(LH)_2$, the chemical shifts belonging to –OH protons in the *vic*-dioxime ligand (LH_2) disappeared after complexation with the Ni(II) ion and the presence of a new resonance at a lower field of 14.34 ppm could be attributed to the formation of the hydrogen bridge, which could be easily identified by deuterium exchange.[23,24] In the ^{1}H-NMR spectra of $[Cd(LH)(H_2O)(Cl)]$ and $[Zn(LH)(H_2O)(Cl)]$, the aromatic ring protons adjacent to the azacrown ether group were observed at 6.37 and 6.68 ppm for $[Cd(LH)(H_2O)(Cl)]$ and at 6.39 and 6.70 ppm for $[Zn(LH)(H_2O)(Cl)]$ as 2 doublets of doublets. These signals, due to azacrown ether moiety, were observed as a multiplet at 3.45-3.55 ppm for $[Cd(LH)(H_2O)(Cl)]$ and at 3.47-3.56 ppm for $[Zn(LH)(H_2O)(Cl)]$. In the ^{1}H-NMR spectra of these complexes, peaks corresponding to N–OH were observed at 10.13 ppm for $[Cd(LH)(H_2O)(Cl)]$ and 10.15 ppm for $[Zn(LH)(H_2O)(Cl)]$. The ^{13}CNMR spectra of the complexes are similar to those of the corresponding *vic*-dioxime. Upon complexation with Ni(II), Cd(II) and Zn(II) cations, the free ligand resonances shifted slightly, as expected. In the FT-IR spectra of the complexes, the strong –NH, C=N and N–O characteristic stretching vibration bands were observed at about 3110-3250 cm^{-1}, 1600-1615 cm^{-1} and 973-983 cm^{-1}, respectively. The FT-IR spectra of $Ni(LH)_2$, $Cu(LH)_2$, and $Co(LH)_2(H_2O)_2$ showed a weak deformation band at 1718-1762 cm^{-1}, indicative of intramolecular hydrogen-bonded bending vibrations (O–H$\cdots$O) that are associated with the square-planar and octahedral *vic*-dioxime complexes.[25] The metal complexes' absorption spectra revealed bands at about 273 nm and 330 nm, which can be assigned to the $\pi \rightarrow \pi^*$ transitions of the aromatic rings and the $n \rightarrow \pi^*$ transitions of the C=N groups, respectively.[18] The molecular weights of all of the complexes were established from the molecular ion peaks observed in the corresponding mass spectra. Most of the complexes showed additional peaks that corresponded to the fragments formed after the loss of the metal ions and the other groups. The fragmentation pattern of the complexes is given as a general scheme showing the main fragmentation paths involved (Figures S3-S7 in Supplementary Materials). Differences in the fragmentation patterns of the *vic*-dioxime complexes are attributed to the effect of the metal ions and geometries. The mass spectra of $[Cd(LH)(H_2O)(Cl)]$ (fragments are based on ^{110}Cd and ^{35}Cl) showed molecular ion peaks at m/z 616.537 $(M\text{-}[H_2O])^+$ (Calc. 616.580), at m/z 472.317 $(MH\text{-}[H_2O{+}CdCl])^+$ (Calc. 472.232), and at m/z 310.072 $(MH\text{-}[H_2O{+}CdCl{+}C_8H_6N_2O_2])^+$ (Calc. 310.189) confirming the formation of the desired compound (Figure S3 in Supplementary Materials). The mass spectra of $[Zn(LH)(H_2O)(Cl)]$ (fragments are based on ^{64}Zn and ^{35}Cl) showed molecular ion peaks at m/z 589.529 $(MH)^+$ (Calc. 589.625), at m/z 472.474 $(MH\text{-}[ZnH_2OCl])^+$ (Calc. 472.232), at m/z 438.332 $(M\text{-}[ZnH_2OCl{+}OOH])^+$ (Calc. 438.227), and at m/z 310.072 $(MH\text{-}[ZnH_2OCl{+}OOH{+}C_8H_5N_2])^+$ (Calc. 310.189) confirming the formation of the desired compound (Figure S4 in Supplementary Materials). The mass spectra of $[Cd(LH)(H_2O)(Cl)]$ and $[Zn(LH)(H_2O)(Cl)]$ showed all of the expected prominent peaks, following the similar proposed fragmentation paths, with a few excep-

tions related to the presence of metal centers. The mass spectra of $Ni(LH)_2$ (fragments are based on ^{58}Ni) showed a molecular ion peak at m/z 1001.769 $(MH)^+$ (Calc. 1001.392) confirming the formation of the desired compound (Figure S5 in Supplementary Materials). The mass spectra of $Cu(LH)_2$ (fragments are based on ^{63}Cu) showed molecular ion peaks at m/z 933.614 (MH-$[CHN_2O_2]$)$^+$ (Calc. 933.382), at m/z 777.406 (MH-$[CHN_2O_2+C_{12}H_{10}]$)$^+$ (Calc. 777.289), and at m/z 631.451 (MH-$[CHN_2O_2+C_{12}H_{10}+CuC_2HN_2O_2]$)$^+$ (Calc. 631.371), confirming the formation of the desired compound (Figure S6 in Supplementary Materials). The loss of 2 water molecules (Figure S7 in Supplementary Materials) after the breaking of the N-Co and -C-C- bonds is a general feature of the prepared Co(II) complex and gives the characteristic peak at m/z 1001.998 (M-$[2H_2O]$)$^+$ (Calc. 1001.382) and at m/z 777.608 (MH-$[2H_2O+C_{14}H_{11}ON_2]$)$^+$ (Calc. 777.287) (fragments are based on ^{59}Co).

Electrochemical measurements

The redox behavior of **1**, LH_2, and its complexes was examined by CV under nitrogen in a DMSO solution with a potential range of 1.0 to –2.5 V versus the Ag/Ag^+ (0.01 M $AgNO_3$) reference electrode. Figure 4a indicates the cyclic voltammogram of both **1** and the LH_2 compounds. As Figure 4a shows, the cyclic voltammogram of **1** displays 2 reversible waves in the positive potential region, between 1.0 and 0.2 V, and only 1 reduction peak in the negative potential region, at around –2.10 V. The main difference in the voltammograms of **1** and LH_2 is that, although **1** displays only 1 reduction peak, at –2.10 V, the LH_2 shows 2 reduction peaks, at –1.83 and –2.17 V, in the negative potential region. Comparison of the redox data of LH_2 with **1** and previously reported oxime-metal complexes[26,27] implies that in the negative potential region, the first reduction process (E_{pc} = –1.83 V) probably corresponds to the oxime moiety, while the second reduction process (E_{pc} = –2.17 V) corresponds to the N-(4-aminophenyl)aza-15-crown-5 moiety. The reversible waves in the positive potential region were always observed for all complexes of LH_2, with small differences in potentials and currents that depend on the stability of the complexes and the kinetics of the electron transfer. The CV measurements show that the Cd(II) and Zn(II) complexes exhibit similar electrochemical behavior, with 2 reduction processes based on either metals or oxime moieties. The M(II)/M(I) and (M:Cd, Zn) reduction processes were obtained at E_{pc} = –1.65 and –1.68 V, and the reduction of oxime moieties was obtained at E_{pc} = –2.03 and –2.11 V for the Cd(II) and Zn(II) complexes, respectively (Figures 4b and 4c). The third peak at –2.27 V in the Cd(II) and Zn(II) voltammograms of these metals corresponds to the azacrown group. The voltammogram of the Ni(II) complex (Figure 4d) showed 3 reduction peaks in the cathodic potential scan, at –1.42 V for Ni(II)/Ni(I), –1.69 V for the oxime, and –2.25 for the azacrown groups of the ligand in the complex (Figure 4d). Figure 4e shows the cyclic voltammogram for the Cu(II) complex, with a cathodic wave for Cu(II)/Cu(I) reduction at $E_{1/2}$ = –0.11 V and a cathodic wave for Cu(I)to-Cu(0) reduction at $E_{1/2}$ =–0.67 V. Comparison of the voltammetric data for the Cu(II) complex with that of the *vic*-dioxime ligand suggests that the reduction peaks at –1.14 V correspond to the oxime-based processes. A reduction peak for the azacrown groups also appears in the voltammogram of the Cu(II) complex, at around –2.10 V. In the cyclic voltammogram of the Co(II) complex, the Co(II)/Co(I) reduction process is obtained at E_{pc} = –1.39 V, with 2 reduction peaks, 1 for oxime moieties at E_{pc} = –1.79 V, and the other at around –2.25 V for the azacrown groups (Figure 4f).

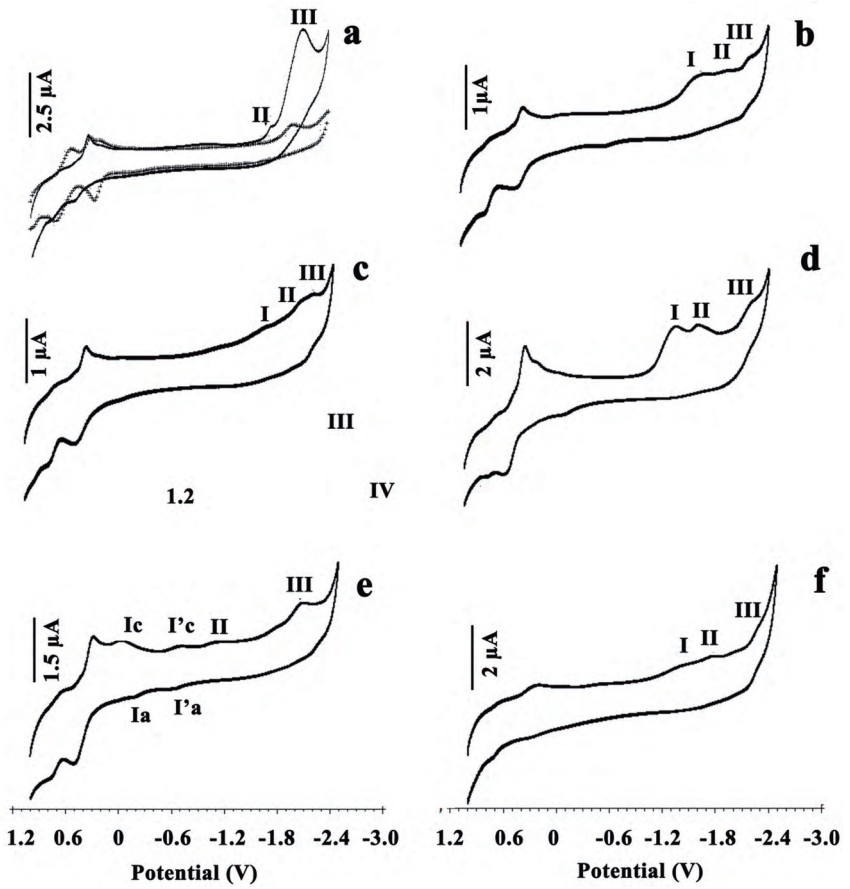

Figure 4. Cyclic voltammograms recorded for the reduction of 1.0 mM: **a)** LH_2 (-) and **1** (**), **b)** $[Cd(LH)(H_2O)(Cl)]$, **c)** $[Zn(LH)(H_2O)(Cl)]$, **d)** $Ni(LH)_2$, **e)** $Cu(LH)_2$, and **f)** $Co(LH)_2(H_2O)_2$ at a GC electrode in DMSO containing 0.1 M TBATFB. Scan rate was 200 mV s^{-1}. I: metal reduction, II: oxime reduction, III: N-(4-aminophenyl)aza-15-crown-5 reduction.

Conclusion

We have described the preparation and characterization of a novel redox active *vic*-dioxime ligand and its Ni(II), Cu(II), Co(II), Cd(II) and Zn(II) metal complexes, which were substituted peripherally with azacrown ether moiety. Spectroscopic analysis confirmed the composition and the structure of the newly obtained compounds. Spectral and microanalysis data for the complexes suggest that the geometry of the $Ni(LH)_2$ and $Cu(LH)_2$ complexes is likely to be square-planar and the geometry of the $Co(LH)_2(H_2O)_2$ complexes octahedral, while the $[Cd(LH)(H_2O)(Cl)]$ and $[Zn(LH)(H_2O)(Cl)]$ complexes are likely to be tetrahedral. Redox behavior was explored using CV, indicating that the metal-centered reduction processes for all of the complexes occurred and that reduction/oxidation potential depends on the structure and conformation of coordination compounds.

Acknowledgments

This work was supported by the Research Fund of Selçuk University Project Number 08101030 under thesis work

Supplementary materials

^{13}C-NMR data and DEPT, ^{1}H-^{13}C HSQC and ^{1}H-^{13}C HMBC correlations of LH_2 (Table S); the numbering of LH_2 for 1D NMR (^{1}HNMR, ^{13}CNMR and DEPT) and 2D NMR (HSQC and HMBC) spectroscopy (Scheme S); UV-Vis spectra of 1.10^{-4} M LH_2 and its metal complexes in DMSO solution (Figure S1); mass spectrum of LH_2 (Figure S2); mass spectrum and mass fragmentation pattern of $[Cd(LH)(H_2O)(Cl)]$ (Figure S3); mass spectrum and mass fragmentation pattern of $[Zn(LH)(H_2O)(Cl)]$ (Figure S4); mass spectrum of $Ni(LH)_2$ (Figure S5); mass spectrum and mass fragmentation pattern of $(Cu(LH)_2)$ (Figure S6); and mass spectrum and mass fragmentation pattern of $(Co(LH)_2(H_2O)_2)$ (Figure S7).

References

1. Gurol, I.; Gumus, G.; Yuksel, F.; Jeanneau, E.; Ahsen, V. *Acta Crystallogr. E* **2006**, *E62*, 3303-3305.
2. Dutta, G.; Kumar, K.; Gupta, B. D. *Organometallics* **2009**, *28*, 3485-3491.
3. Meshram, H. M.; Eeshwaraiah, B.; Sreenivas, M.; Aravind, D.; Syama Sundar, B.; Yadav, J. S. *Synthetic Commun.* **2009**, *39*, 1857-1863.
4. Gupta, B. D.; Yamuna, R.; Mandal, D. *Organometallics* **2006**, *25*, 706-714.
5. Kantekin, H.; Bakaray, A.; Bıyıklıoğlu, Z.; Kılıçaslan, M. B. *Trans. Met. Chem.* **2008**, *33*, 161-165.
6. Musilova, L.; Kuca, K.; Jung, Y. S.; Jun, D. *Clin. Toxicol.* **2009**, *47*, 545-550.
7. Bilgin, A.; Ertem, B.; Ağın, F. D.; Gök, Y.; Karslıoğlu, S. *Polyhedron* **2006**, *25*, 3165-3172.
8. Guzel, B.; Avşar, G.; Çınkır, H. F. *Synth. React. Inorg. Met.-Org. Chem.* **2007**, *37*, 801-804.
9. Derelanko, M. J.; Rusch, G. M. *Drug Chem. Toxicol.* **2008**, *31*, 97-114.
10. Yılmaz, A.; Taner, B.; Deveci, P.; Yılmaz Obalı, A.; Arslan, U.; Şahin, E.; Uçan, H. İ.; Özcan, E. *Polyhedron* **2010**, *29*, 2991-2998.
11. Koroglu, M. A.; Erol, I.; Korcan, E.; Konuk, M. J. *Macromol. Sci. A* **2007**, *44*, 817-830.
12. Demetgül, C.; Serin, S. *Carbohyd. Polym* **2008**, *72*, 506-512.
13. Karapinar, E.; Karapinar, N.; Ozcan, E.; Coskun, A. *Synth. React. Inorg. Met.-Org. Chem.* **2007**, *37*, 611-619.
14. Kantekin, H.; Bakaray, A.; Bıyıklıoğlu, Z. *Trans. Met. Chem.* **2007**, *32*, 209-213.
15. Taner, B.; Deveci, P.; Bereket, S.; Solak, A. O.; Özcan, E. *Inorg. Chim. Acta* **2010**, *363*, 4017-4023.
16. Lu, X. X.; Qin, S. Y.; Zhou, Z. Y.; Yam, V. W. W. *Inorg. Chim. Acta* **2003**, *346*, 49-56.
17. Uçan, H. İ.; Mirzaoğlu, R. *Synth. React. Inorg. Met.-Org. Chem.* **1990**, *20*, 437-449.
18. Ünver, H.; Hayvali, Z. *Spectrochim. Acta A* **2010**, *75*, 782-788.

19. Kilic, A.; Tas, E.; Gumgum, B.; Yilmaz, I. *J. Coord. Chem.* **2007**, *60*, 1233-1246.
20. Tas, E.; Kara, H.; Durgun, M.; Kilic, A.; Yilmaz, I. *Synth. React. Inorg. Met.-Org. Chem.* **2009**, *39*, 379-387.
21. Coşkun, A.; Karapinar, E. *J. Incus. Phenom. Mol.* **2008**, *60*, 59-64.
22. Yuksel F.; Gürek, A. G.; Durmuş, M.; Gürol, İ.; Ahsen, V.; Jeanneau, E.; Luneau, D. *Inorg. Chim. Acta* **2008**, *361*, 2225-2235.
23. Mandal, D.; Gupta, B. D. *Organometallics* **2006**, *25* 3305-3307.
24. Bhuyan, M.; Laskar, M.; Gupta, B. D. *Organometallics* **2008** *27*, 594-601.
25. Uçar, A.; Deveci, P.; Taner, B.; Fındık, M.; Bereket, S.; Özcan, E.; Solak, A. O. *J. Coord. Chem.* **2010**, *63*, 3083-3092.
26. Deveci, P.; Taner, B.; Kılıç, Z.; Solak, A. O.; Arslan, U.; Özcan, E. *Polyhedron* **2011**, *30*, 1726-1731.
27. Kandaz, M.; Koca, A.; Özkaya, A. R. *Polyhedron* **2004**, *23*, 1987-1996.

Suplementary Materials

Table S. ^{13}C NMR data and DEPT, $^{1}H–^{13}C$ HSQC and $^{1}H–^{13}C$ HMBC correlations of LH_2.

Carbon number	Chemical shift	DEPT	$^{1}H–^{13}C$ HSQC	$^{1}H–^{13}C$ HMBC
	δC(ppm)		(^{1}J)	(^{2}J)-(^{4}J)
1	57.30	CH_2	3.37(H_1)	3.54(H_2)
2	73.40	CH_2	3.54(H_2)	3.37(H_1), 3.46(H_3)
3	74.43	CH_2	3.46(H_3)	3.50(H_4), 3.54(H_2)
4	74.86	CH_2	3.50(H_4)	3.46(H_3), 3.50(H_5)
5	75.64	CH_2	3.50(H_5)	3.50(H_4)
6	148.90	C	-	6.70(H_7), 6.37(H_8), 3.37(H_1)
7	116.61	CH	6.70(H_7)	6.37(H_8)
8	128.92	CH	6.37(H_8)	6.70(H_7), 7.69(H_{16})
9	132.94	C	-	6.70(H_7),6.37(H_8),7.69(H_{16}),7.42-7.40(H_{13})
10	153.81	C	-	7.69(H_{16}), 7.42-7.40(H_{13}), 10.13(H_{18}), 11.54(H_{17})
11	154.01	C	-	7.69(H_{16}), 7.42-7.40(H_{13}), 7.26-7.28($H_{14,15}$), 10.13(H_{18}), 11.54(H_{17})
12	136.80	C	-	7.69(H_{16}), 7.42-7.40(H_{13}), 7.26-7.28($H_{14,15}$)
13	134.42	CH	7.42-7.40 (H_{13})	7.69(H_{16}),7.26-7.28($H_{14,15}$)
14	134.34	CH	7.26-7.28 (H_{14})	7.69(H_{16}), 7.42-7.40(H_{13}), 7.26-7.28(H_{15})
15	136.90	CH	7.26-7.28 (H_{15})	7.69(H_{16}), 7.42-7.40(H_{13}), 7.26-7.28(H_{14})

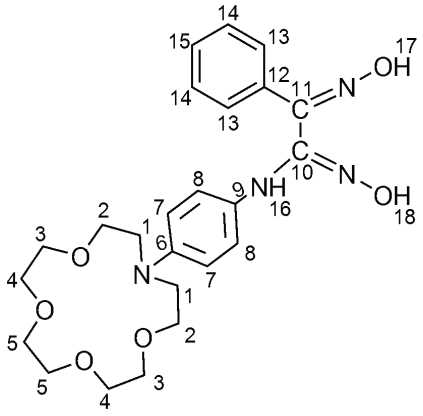

Scheme S

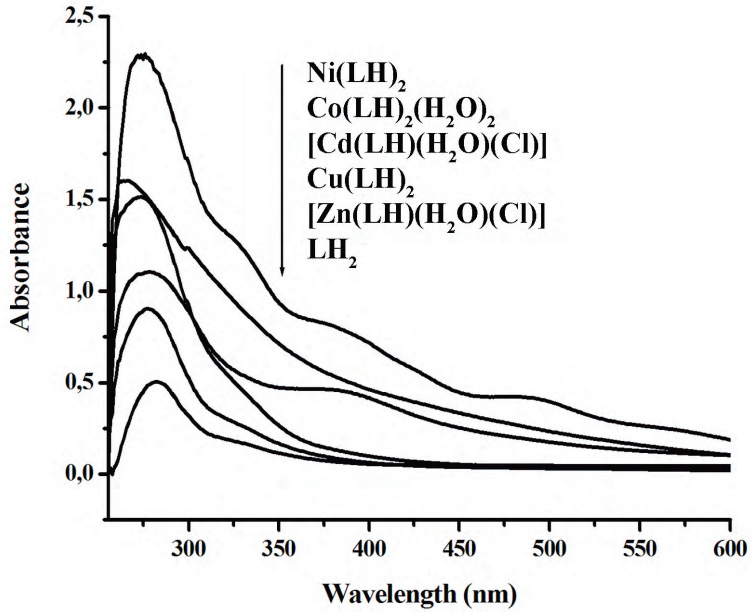

Figure S1. UV-Vis spectra of 1.10^{-4} M LH_2 and its metal complexes in DMSO solution.

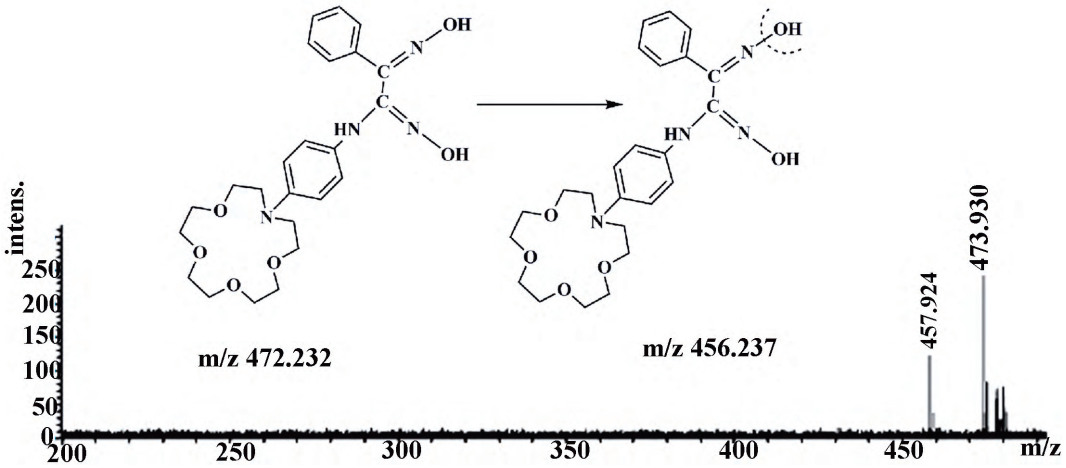

Figure S2. Mass spectrum of the LH_2.

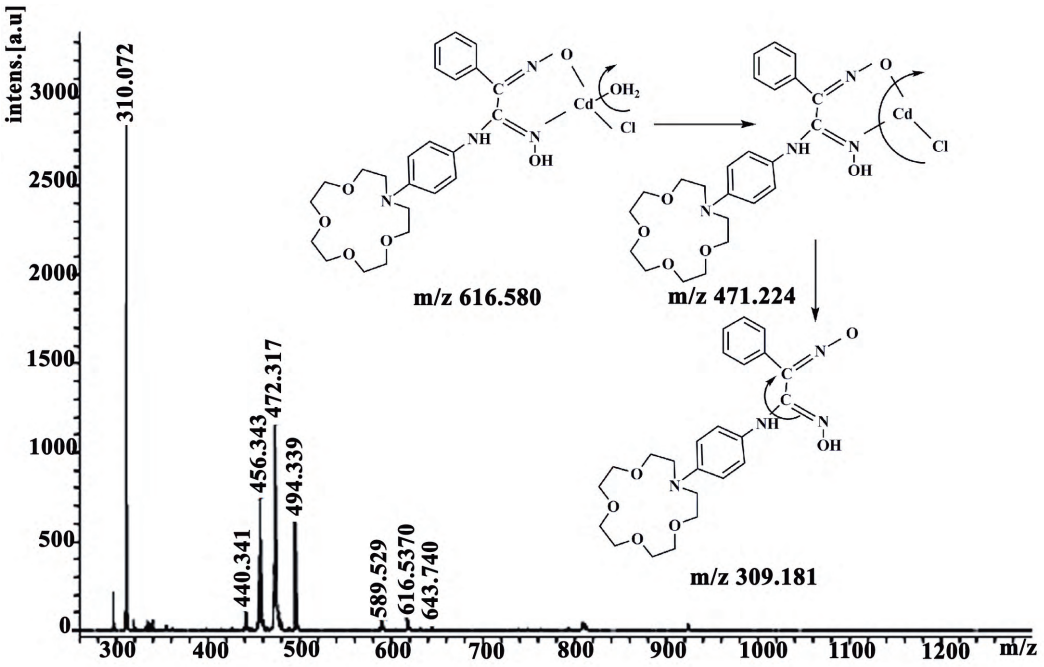

Figure S3. Mass spectrum and mass fragmentation pattern of the [Cd(LH)(H_2O)(Cl)].

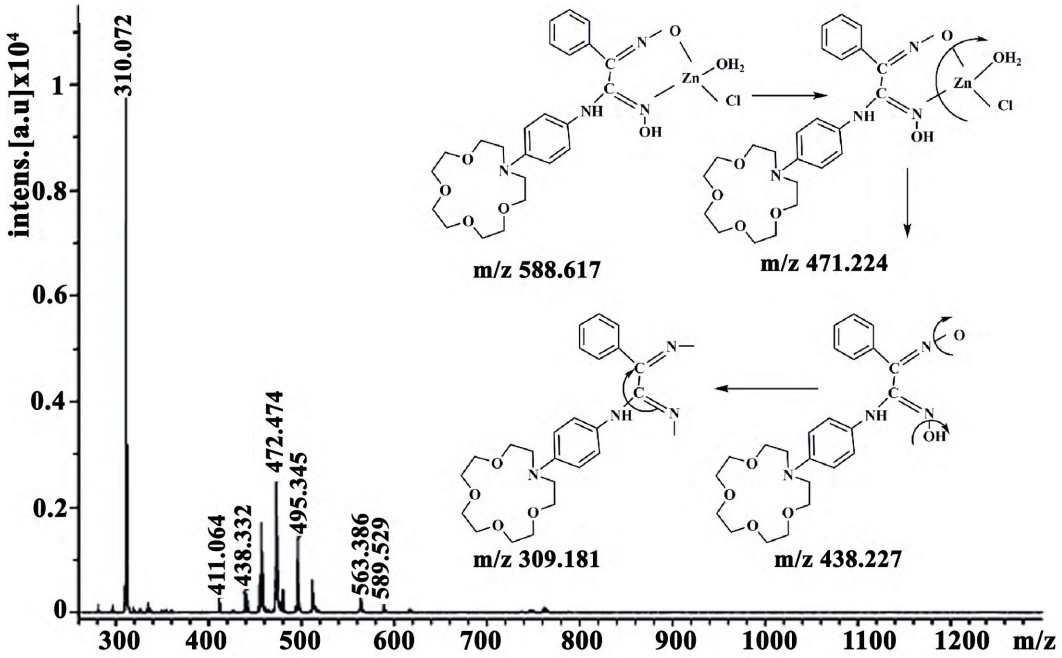

Figure S4. Mass spectrum and mass fragmentation pattern of the [Zn(LH)(H_2O)(Cl)].

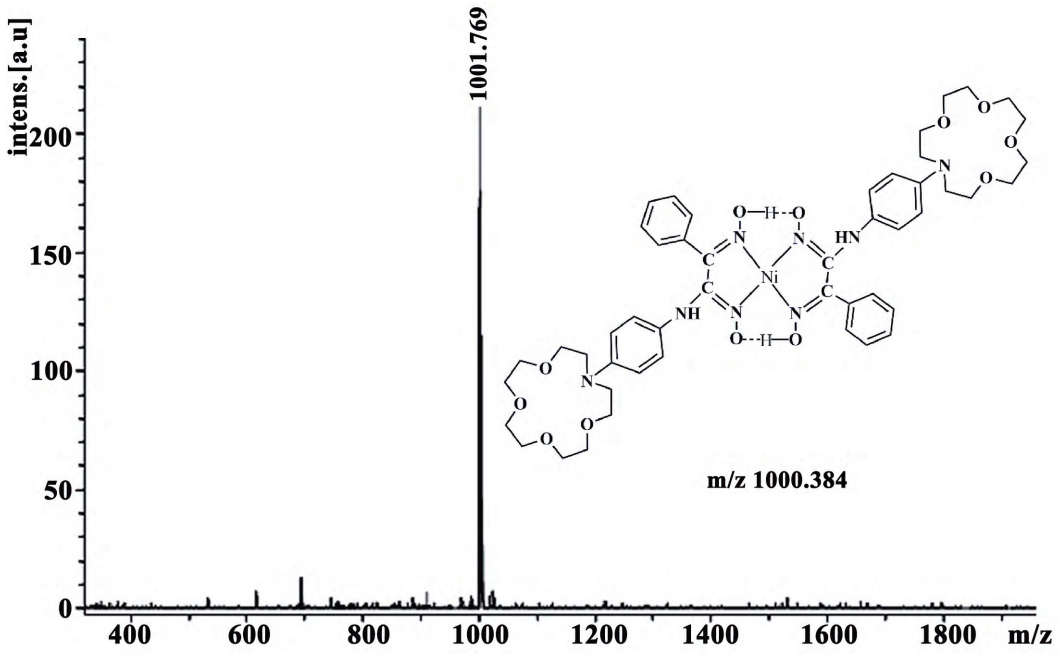

Figure S5. Mass spectrum of the $Ni(LH)_2$.

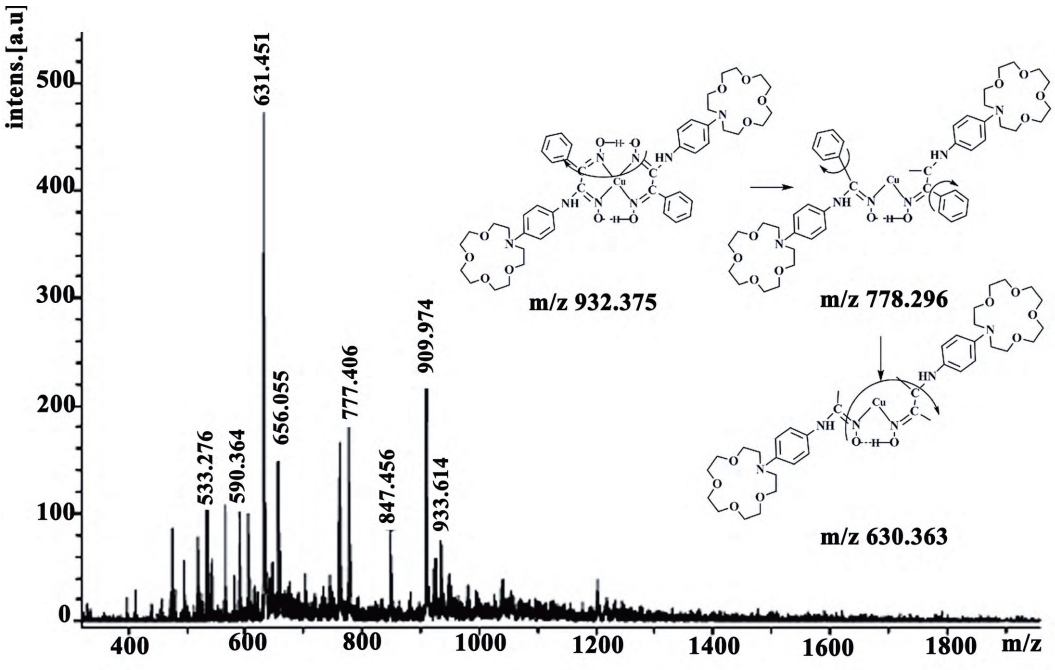

Figure S6. Mass spectrum and mass fragmentation pattern of the ($Cu(LH)_2$).

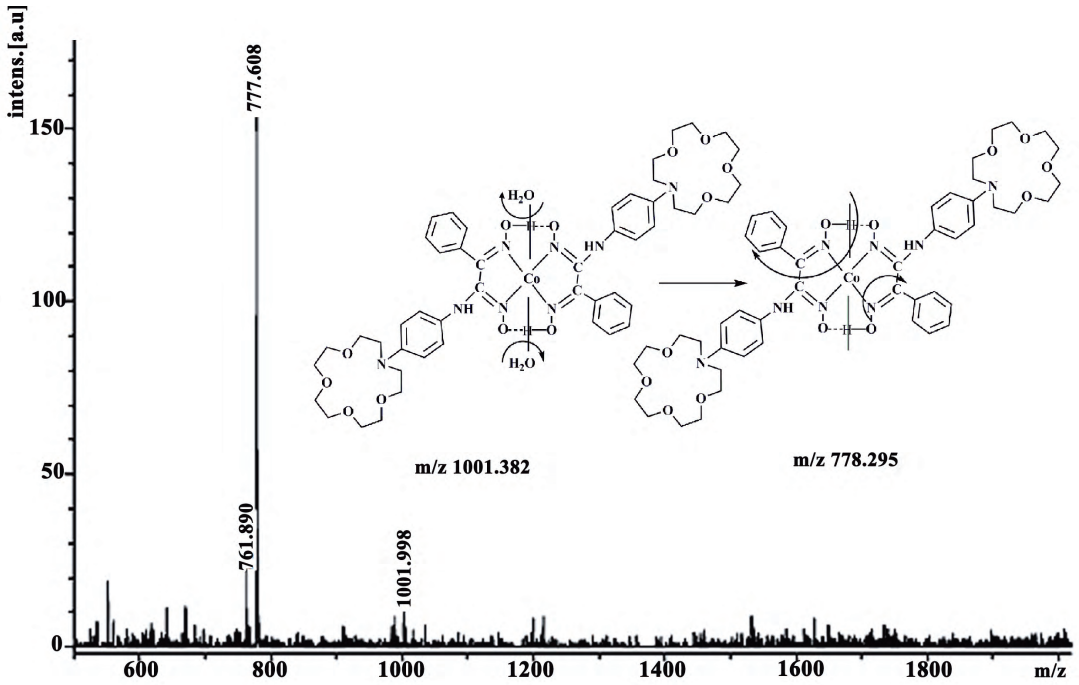

Figure S7. Mass spectrum and mass fragmentation pattern of the Co(II) complex ($Co(LH)_2(H_2O)_2$).